AD-A073 792 ROCKWELL INTERNATIONAL THOUSAND OAKS CA SCIENCE CENTER F/G 9/1
HETEROJUNCTION MATERIALS AND CHARACTERISTICS.(U)
MAY 79 D L MILLER, J S HARRIS N00014-78-C-0330

UNCLASSIFIED SC5158.2FR NL

1 OF 1

END

DATE FILMED 10-78

DDC

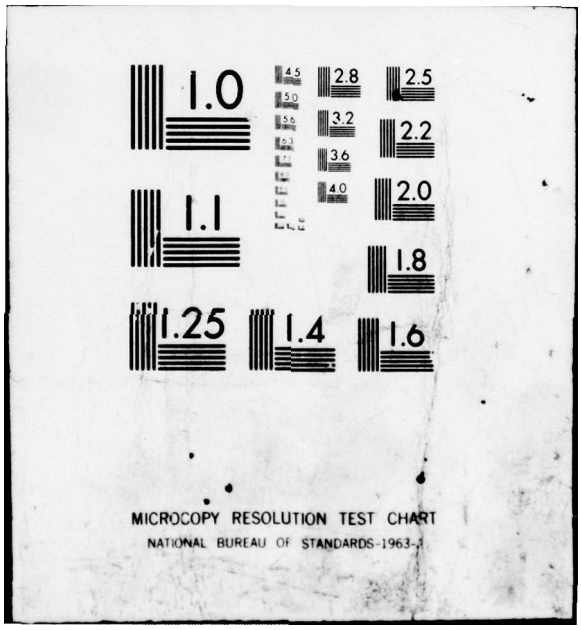
1.0
1.1
1.25
1.4
1.6
1.8
2.0
2.2
2.5
2.8
3.2
3.6
4.0
4.5
5.0
5.6
MICROCOPY RESOLUTION TEST CHART
NATIONAL BUREAU OF STANDARDS-1963-A

(12) LEVEL II

10

May, 1979

SC5158.2FR

HETEROJUNCTION MATERIALS AND CHARACTERISTICS

Final Report

By

D. L. Miller and J. S. Harris, Jr.

Prepared under Contract No. N00014-78-C-0330
Project No. NR-373-027(427)

By

ROCKWELL INTERNATIONAL ELECTRONICS RESEARCH CENTER
Thousand Oaks, California 91360

For

Electronic and Solid State Sciences Program
Physical Sciences Division
Office of Naval Research
Department of the Navy
800 North Quincy Street
Arlington, VA 22217

AD A073792

DDC FILE COPY

Approved by:

J. S. Harris, Jr.
Program Manager

Approved for public release; distribution unlimited.

Rockwell International

UNCLASSIFIED

SECURITY CLASSIFICATION OF THIS PAGE (When Data Entered)

REPORT DOCUMENTATION PAGE

READ INSTRUCTIONS BEFORE COMPLETING FORM

1. REPORT NUMBER	2. GOVT ACCESSION NO. / 3. RECIPIENT'S CATALOG NUMBER
4. TITLE (and Subtitle): Heterojunction Materials and Characteristics.	5. TYPE OF REPORT & PERIOD COVERED: Final Report for period 03/01/78 through 02/28/79
	6. PERFORMING ORG. REPORT NUMBER: SC5158.2FR
7. AUTHOR(s): D.L. Miller and J.S. Harris	8. CONTRACT OR GRANT NUMBER(s): N00014-78-C-0330 Project No. NR 373-027(427)
9. PERFORMING ORGANIZATION NAME AND ADDRESS: Rockwell International Electronics Research Center, 1049 Camino Dos Rios, Thousand Oaks, California 91360	10. PROGRAM ELEMENT, PROJECT, TASK AREA & WORK UNIT NUMBERS: 12 39 p.
11. CONTROLLING OFFICE NAME AND ADDRESS: Office of Naval Research, 800 North Quincy Street, Arlington, VA 22217	12. REPORT DATE: May 1979
	13. NUMBER OF PAGES: 24
14. MONITORING AGENCY NAME & ADDRESS (if different from Controlling Office)	15. SECURITY CLASS. (of this report): Unclassified
	15a. DECLASSIFICATION/DOWNGRADING SCHEDULE

16. DISTRIBUTION STATEMENT (of this Report)

Approved for public release; distribution unlimited

9 Final rept. 1 Mar 78-28 Feb 79.

17. DISTRIBUTION STATEMENT (of the abstract entered in Block 20, if different from Report)

18. SUPPLEMENTARY NOTES

19. KEY WORDS (Continue on reverse side if necessary and identify by block number)

Heterojunction, molecular beam epitaxy, GaAs, GaAlAs

20. ABSTRACT (Continue on reverse side if necessary and identify by block number)

Molecular beam epitaxy was used to provide samples for extremely abrupt GaAs/GaAlAs heterojunctions for AES profiling of the interface and ESCA measurements of the AlAs valence band structure. The latter samples consist of MBE AlAs layers covered with 50Å to 100Å of GaAs as protection against oxidation.

MBE growth of n-type AlGaAs was studied also. N-type AlGaAs was produced although all the n-type conducting AlGaAs layers grown by MBE had low activation of the dopant (2%-40%) and relatively low room temperature mobilities (650cm²/v-sec to 1200cm²/v-sec).

DD FORM 1 JAN 73 1473 EDITION OF 1 NOV 65 IS OBSOLETE

Cu CM SQ

UNCLASSIFIED

SECURITY CLASSIFICATION OF THIS PAGE (When Data Entered)

389 949

It was found that Al source design and background vacuum were important influences on the quality of n-type AlGaAs produced.

Some initial measurements were made on the electrical properties of n-GaAs/n-AlGaAs and n-GaAs/n-AlGaAs/n-GaAs structures. I-V measurements on n-n structures at room temperature showed no deviations from ohmic behavior, while C-V measurements on n-n-n structures were hampered by trapping effects in the AlGaAs.

TABLE OF CONTENTS

LIST OF FIGURES

1.0 INTRODUCTION

Heterojunctions of III-V compounds have long been of technological interest, and more recently have been the subject of a wide range of theoretical and experimental treatments. Particularly, the roles of the microscopic properties of the heterojunctions, such as interfacial bonding, atomic redistribution, and interface-related defect distributions, have been recognized to be extremely important. Experiments such as Auger profiling, XPS, and UPS have been utilized to investigate the physical and electronic nature of the heterojunction on an atomic scale, while experiments concerned with carrier confinement at potential wells produced by heterojunction band discontinuities attest to the validity of present models of heterojunction band behavior. Some of these experiments have been made possible only by the use of molecular beam epitaxy (MBE) to grow the necessary atomically abrupt junctions.

Despite this progress, a consistent and complete picture of heterojunction properties has yet to emerge, and in some cases it is not known whether experimental discrepancies are due to differences in growth techniques or to fundamental differences in what each experiment observes. For example, in experiments where photoresponse is measured or carrier confinement in potential wells is observed, experiments have shown agreement with simple models which derive band edge behavior based on Poisson's equation and knowledge of band edge energies in bulk material. Such models predict an observable barrier in GaAs(n)-GaAlAs(n) heterojunctions, for example. Transport experiments, however, have failed to confirm the predicted rectification except in one recent experiment in which material with an extremely low doping density was used[1].

The intent of this contract is to use molecular beam epitaxy (MBE) to aid in the investigation of some of the fundamental properties of some heterojunctions which are of technological interest, namely junctions

in the AlGaAs/GaAs and Ge/GaAs systems. Since the abruptness of the heterojunctions can have a profound effect on its properties, it is anticipated that the use of MBE to grow extremely abrupt junctions can lead to a clearer understanding of the basic nature of such junctions. As discussed above, the general absence of rectification in a GaAs(n)/AlGaAs(n) heterojunction is not understood, and may arise from effects due to the nature of the material growth techniques used to form the junction. The use of MBE to form metallurgically ideal junctions could help to explain this phenomenon.

This report contains in section 2 a discussion of the technical work done, including technical difficulties encountered with the material system which was explored (AlGaAs/GaAs). The results and recommendation for future work are summarized in section 3.

2.0 TECHNICAL DISCUSSION

In this section, we outline the technical aspects of the project. First, we discuss the material systems and experiments which were attempted. We then discuss the results which were obtained.

2.1 Project Outline

At the outset of this project, three areas were considered for investigation of heterojunction properties. All of these were chosen to take advantage of the extremely abrupt junctions obtainable by MBE, and to apply MBE to heterojunction experiments of current interest. These areas were: 1) investigation of the growth of Ge/GaAs heterojunctions, and the electrical characterization of the Ge on GaAs epilayers and interfaces, 2) growth of AlAs/GaAs heterojunctions suitable for ESCA measurements of the valence band discontinuity in the GaAs/AlAs system, 3) investigation of the existence of a conduction band spike in the GaAs(n)/AlGaAs(n) heterojunction in light of the commonly observed lack of rectification in this junction.

2.2 Investigation of Ge/GaAs Heterojunctions

Only a small amount of work was done with this system for several reasons. The first reason was that our experience previous to this contract had shown that Ge layers grown on GaAs had high carrier concentration ($n \cong 10^{18}/cm^3$), presumably due to As doping of the Ge layer. This limited the type of measurements which could be made on Ge/GaAs heterojunctions. The second reason was that Ge is an n-type dopant for GaAs (under As-rich growth conditions) and experience had shown that deposition of large amounts of dopant material in the MBE chamber could cause high background doping in subsequent GaAs epilayers. Therefore Ge layer growth received low priority. Finally, most of the impetus for studying Ge/GaAs heterojunctions

came from another ONR contractor who was unable to make use of any Ge/GaAs epilayers until late in our contract year.

Some work was done in preparation for growing Ge epilayers on GaAs. A new Ge source was constructed, and one Ge epilayer was grown on GaAs. This layer was heavily contaminated by gallium which had accidentally been transferred from the chamber LN_2 shrouding to the source thermal radiation shielding during source loading. The source was subsequently cleaned and reloaded, but no further Ge growths were made before the end of the contract period.

2.3 Investigation of the GaAs/AlGaAs System

Essentially all the effort of this contract was directed toward understanding the GaAs/AlGaAs system. Layers were grown for experiments to determine the abruptness of the GaAs/AlGaAs heterojunction (in conjunction with Prof. Spicer's group at Stanford University), for experiments to determine valence band edge discontinuities (in conjunction with Ron Grant, Science Center), and for our own efforts to look for rectification in GaAs(n)/AlGaAs(n) heterojunctions (with measurements made in conjunction with Prof. H. Kroemer at U.C.S.B.). Table 1 lists all the MBE layers grown for this series of experiments. Technical details of each experiment are given here.

2.3.1 GaAs/GaAlAs Heterojunction Abruptness Studies

Two MBE growths were made early in the project for Mr. Mike Garner at Stanford University (Prof. William Spicer's group) to investigate the heterojunction width by sputter-etch profiling, using Auger electron spectroscopy (AES) to observe the junction. Both samples were grown with a thin MBE AlGaAs layer on top of an MBE GaAs layer about 1μm thick. In the first sample, the 600Å thick $Al_{.8}Ga_{.2}As$ layer was found by AES to be oxidized through. The second sample had an $Al_{.5}Ga_{.5}As$ layer 150±20Å thick and was successfully used for AES profiling of the interface region.

TABLE 1

Layer #	Composition	Doping (Concentration)	Comments
2696-11.2	GaAs(Sn)/GaAs(Be)/$Ga_{.2}Al_{.8}As$(Be)	Be	MBE solar cell, also for AES profiling, oxidized
102	GaAs(Sn)/$Ga_{.5}Al_{.5}As$(Sn)	Sn($10^{16}/cm^3$)	AES profiling; width ~12Å
112	$Ga_{.95}Al_{.05}As$		Composition calibration (photoluminescence)
113	$Ga_{.89}Al_{.11}As$		Composition calibration (photoluminescence)
124	GaAs/AlAs/GaAs	Sn($2x10^{16}/cm^3$)	On (111), (110), (100) for R. Grant ESCA
125	$Ga_{.87}Al_{.13}As$(Sn)/GaAs(Sn)	Sn($4x10^{16}/cm^3$)	Doping of AlGaAs -- high ρ
126	$Ga_{.87}Al_{.13}As$(Sn)/GaAs(Sn)	Sn($1x10^{17}/cm^3$)	Doping of AlGaAs -- high ρ
127	$Ga_{.87}Al_{.13}As$(Sn)/GaAs(Sn)	Sn($6x10^{17}/cm^3$)	Doping of AlGaAs -- high ρ
137	$Ga_{.90}Al_{.10}As$		Composition calibration (photoluminescence)
138	$Ga_{.88}Al_{.12}As$		Composition calibration (photoluminescence)
139	$Ga_{.79}Al_{.21}As$		Composition calibration (photoluminescence)
140	$Ga_{.94}Al_{.06}As$(Sn)/GaAs(Sn)	Sn($5x10^{16}/cm^3$)	Doped AlGaAs, high ρ
141	$Ga_{.96}Al_{.04}As$(Sn)/GaAs(Sn)	Sn($2x10^{17}/cm^3$)	Doped AlGaAs, ρ_{300} = $1.7x10^6$ Ω-cm
143	$Ga_{.98}Al_{.02}As$(Sn)/GaAs(Sn)	Sn($1x10^{17}/cm^3$)	Doped AlGaAs, ρ_{300} = $2.4x10^6$ Ω-cm

SC5158.2FR

TABLE 1 (Cont.)

Layer #	Composition	Doping (Concentration)	Comments
152	$Ga_{.95}Al_{.05}As(Sn)$	$Sn(2x10^{17}/cm^3)$	Doped AlGaAs, high ρ
159	$Ga_{.98}Al_{.02}As(Ge)$	$Ge(1x10^{18}/cm^3)$	Doped AlGaAs, $n_d = 5x10^{16}$, $\mu_{300} = 846$
165	$Ga_{.8}Al_{.2}As(Ge)$	$Ge(1x10^{18}/cm^3)$	Doped AlGaAs, high ρ
166	$Ga_{.9}Al_{.1}As(Ge)$	$Ge(1x10^{16}/cm^3)$	Doped AlGaAs, high ρ
167	$Ga_{.9}Al_{.1}As(Sn)/GaAs(Sn)$	$Sn(1x10^{17}/cm^3)$	Doped AlGaAs, high ρ
195	AlGaAs (three compositions)		calib., not measured
196	AlGaAs (three compositions)	$Sn(4x10^{16}/cm^3)$	High ρ(all compositions)
198	AlGaAs		New source test
199	$Ga_{.8}Al_{.2}As/GaAs$	$Sn(5x10^{16}/cm^3)$	Doped AlGaAs with new source -- high ρ
206	AlGaAs(Sn)/GaAs(Sn) (three comp.)	$Sn(2x10^{18}/cm^3)$	First n-type AlGaAs above 2% Al.
207	AlGaAs(Sn)/GaAs(Sn) (three comp.)	$Sn(2x10^{18}/cm^3)$	Conducting AlGaAs(Sn).
214	GaAs/AlAs/GaAs		On (110), (111),(100), for R. Grant,ESCA
218	GaAlAs		Composition calibration
223	$Al_{.3}Ga_{.7}As(Sn)/GaAs(Sn)$	$Sn(5x10^{17}/cm^3)$	Conducting AlGaAs n-n
224	$GaAs(Sn)/Al_{.3}Ga_{.7}As(Sn)/GaAs(Sn)$	$Sn(5x10^{17}/cm^3)$	Conducting AlGaAs n-n-n, H_2 gas background
241	GaAs/AlAs/GaAs		On (110), for R. Grant, ESCA

This layer was found to be abrupt on the scale of instrument resolution (10-15Å), with a junction depth of 140Å[2]. A depth profile of the Al LVV Auger signal is shown in Fig. 1.

2.3.2 GaAs/AlAs Valence Band Discontinuity Studies

Three sample were grown by MBE for ESCA studies of the valence band discontinuity at the GaAs/AlAs heterojunction. These samples were delivered to Dr. R. Grant at the Science Center and the results of his measurements are reported under his ONR contract. These samples consisted of substrate GaAs, 1μm of GaAs buffer layer, 0.5μm AlAs, and a covering layer of 50Å to 100Å GaAs. The thin GaAs layer is used to prevent oxidation of the AlAs while allowing sputter cleaning of the AlAs surface. These samples were grown on (110), (111) and (100) oriented GaAs, to allow angular effects in the ESCA spectrum to be determined. These samples are now being used for ESCA experiments and appear to be satisfactory.

2.3.3 GaAs/GaAlAs Heterojunction Characterization

By far the largest effort on this contract was expended on the material growth aspects of this heterojunction. The structure which was to be grown was a GaAs(n)/GaAlAs(n)/GaAs(n) double heterojunction. It was planned to grow this structure with doping appropriate for C-V profiling of both interfaces. This was to be done in conjunction with Prof. H. Kroemer of U.C.S.B. Also, measurements would be made of GaAs(n)/GaAlAs(n) heterojunctions to look for evidence of a rectifying spike in the GaAlAs conduction band.

A large amount of effort was spent in developing techniques to produce MBE n-type AlGaAs suitable for these structures. Initial attempts at producing n-type AlGaAs produced high resistivity material. For example, sample 141 (see Table 1) was grown with only 4% Al, and a Sn dopant flux sufficient to give $2 \times 10^{17}/cm^3$, yet the resistivity of the layer was measured to be about 2×10^6 Ω-cm at room temperature.

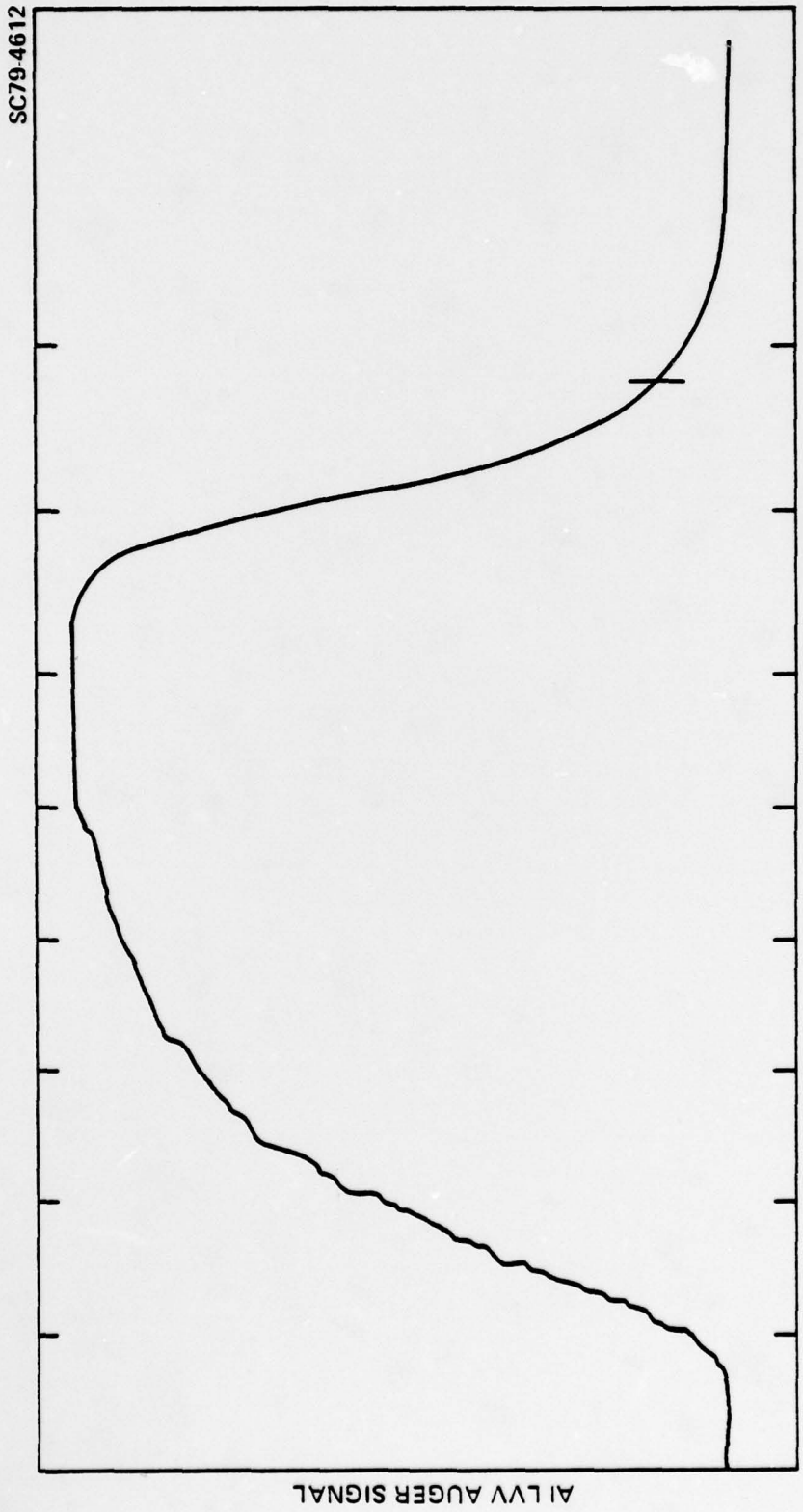

SC5158.2FR

Fig. 1. Depth profile of an Auger Al LVV line in an AlGaAs/GaAs heterojunction. Ion beam energy is 500eV, which gives a depth resolution of about 10-15Å.

A number of measures were taken which resulted in low resistivity material. The first steps were to reduce the background of H_2O, CO, and CO_2 present in the chamber during growth. To do this, the shroud surrounding the sources was changed from water cooling to liquid nitrogen cooling. This change meant that only LN_2 cooled surfaces and the sources themselves were in line-of-sight of the substrate during growth. Additionally, a 10°K cryogenic pump was purchased with Rockwell capital equipment funds to add pumping speed for CO. These figures served to reduce background contaminants significantly. Figures 2 and 3 are mass spectrometer scans taken during the growth of samples 141 (high resistivity) and 206 (our first successful low resistivity n-type AlGaAs growth). Although the mass spectrometer sensitivity varied some with time, exposure to various atmospheres, and the exact positioning of the substrate holder, these traces were chosen to be representative of the amount of background reduction produced by the steps outlined above.

Despite these background gas reductions, the AlGaAs grown was still high resistivity material. Various As/Ga ratios and substrate temperatures were used, with no success. Evidence suggested that the Al (and perhaps Ga) sources were a partial cause of this. Background CO, although reduced in general from previous levels, continued to be very sensitively dependent on the preparation and degassing of the Al source. Figure 4 is a mass spectrometer trace taken during growth of epilayer 196, which was high resistivity AlGaAs. It can be seen that there was significantly more CO, CO_2, CH_4, and H_2O present during this layer growth. Therefore a new design was employed for the Al and Ga sources.

The newly designed Al and Ga sources were basically similar to previous designs, but used a flanged pyrolytic boron nitride crucible instead of a straight sided crucible as before. This eliminated any direct or nearly direct paths from the hot heater filament area to the substrate. In retrospect, this was probably the most significant improvement to the MBE system, since Al_2O and AlO has been detected by other

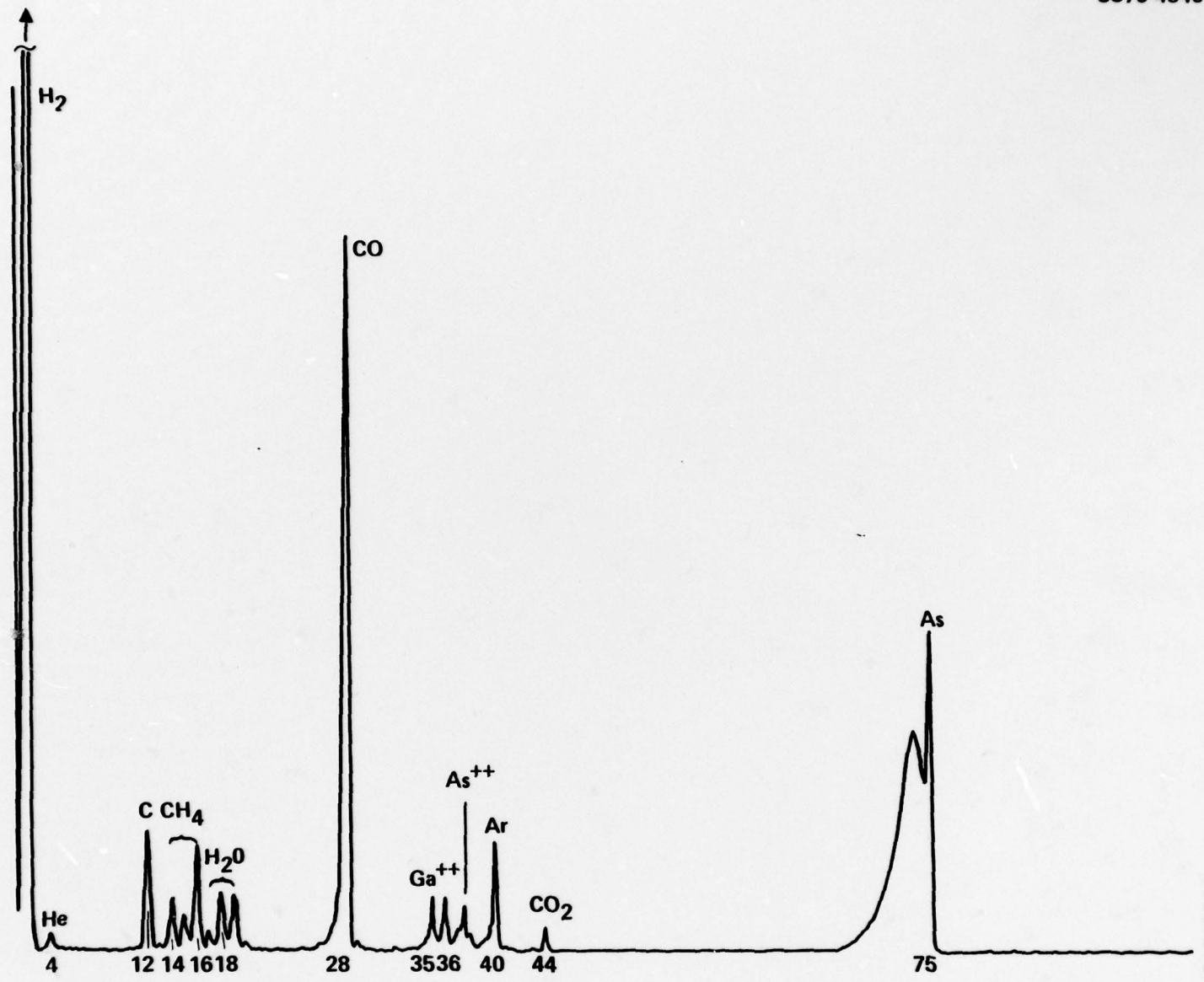

Fig. 2. Mass spectrometer scan taken during the growth of layer 141, which was high resistivity $Al_{.04}Ga_{.96}As$.

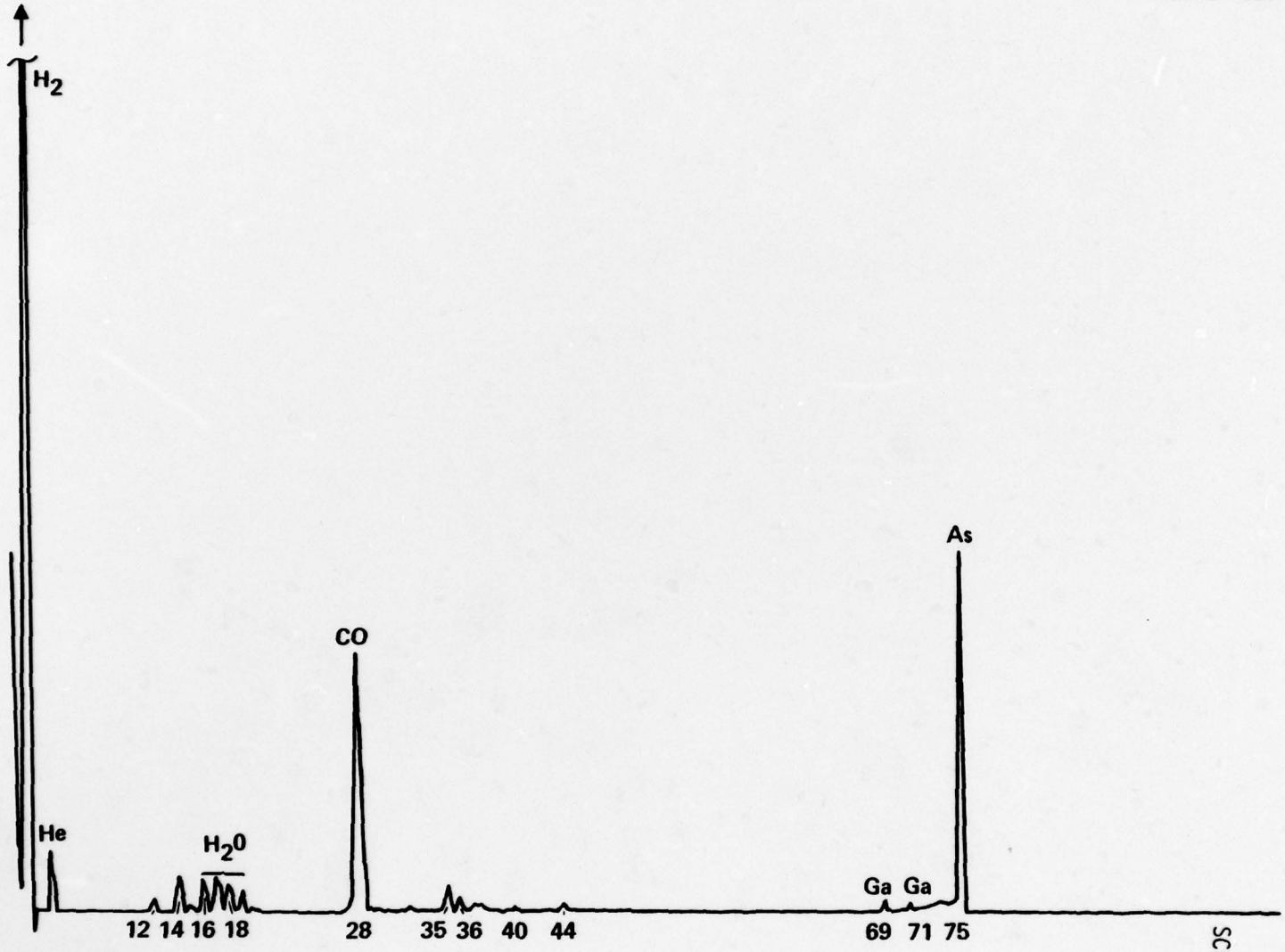

Fig. 3. Mass spectrometer scan taken during the growth of layer 206, which was conducting n-type $Al_{.3}Ga_{.7}As$.

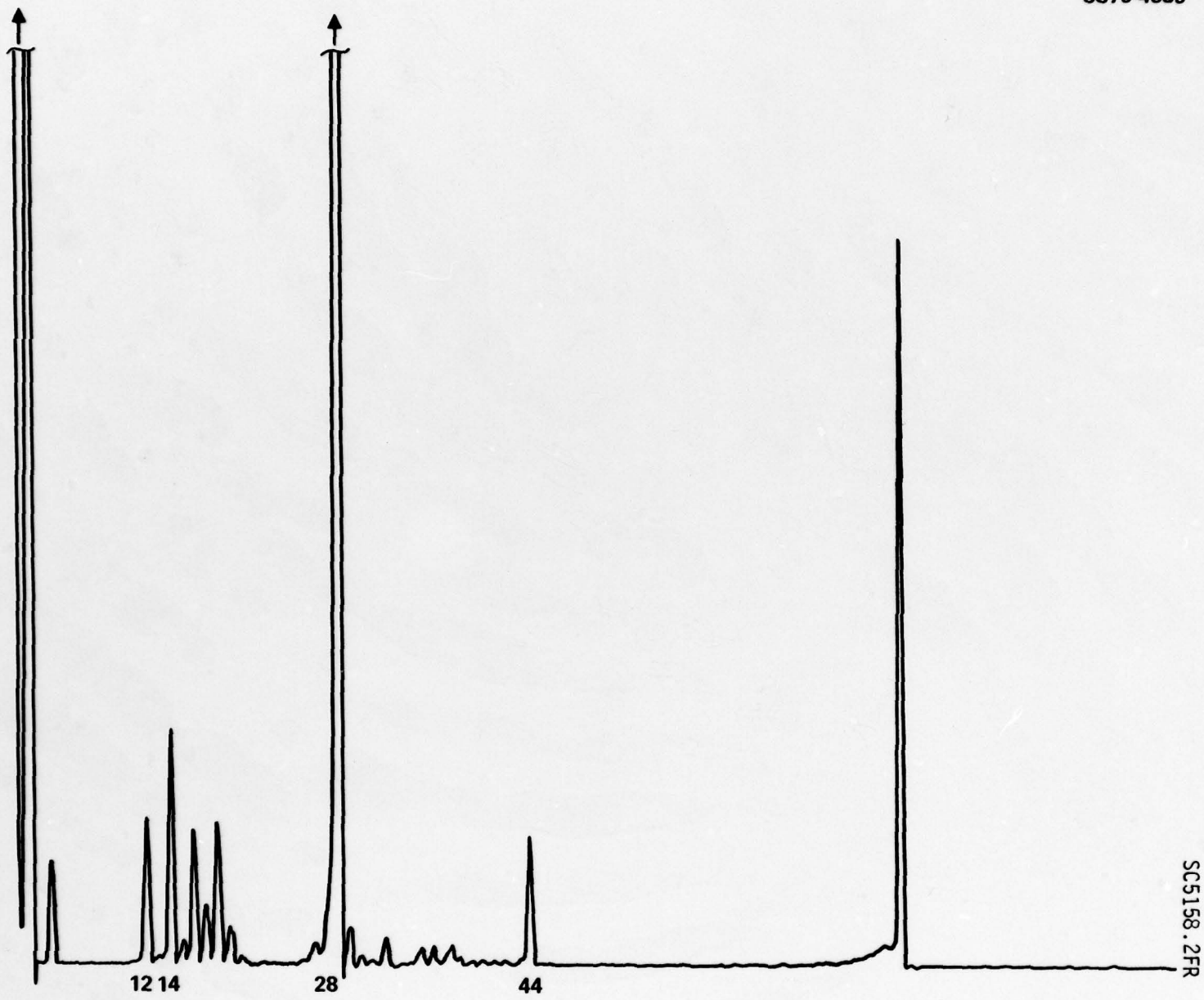

Fig. 4. Mass spectrometer scan taken during the growth of layer 196, which was high resistivity AlGaAs.

researchers from a source with construction similar to our first design operating at about the same temperature[3]. This was reported to be due to reduction of Al_2O_3 by the Ta heater wires.

Another factor which contributed to the difficulty in producing conducting n-type AlGaAs was the instability experienced with the Sn doping source. Several doping runs were attempted in which the Sn flux was calculated to give $>10^{18}/cm^3$ dopant concentration in the AlGaAs layer, but which were later found to have received much less Sn. It was eventually discovered that running the Sn source at elevated temperatures caused a drastic change in calibration, and that often the dopant flux had been an order of magnitude lower than intended. In view of the low activation of Sn in GaAlAs, this factor may have prevented the successful production of conducting n-type GaAlAs in a number of early runs.

Figure 5 shows a plot of electron Hall mobility as a function of doping density for two growths which produced conducting AlGaAs. These growths were done with a constant Sn dopant flux, while the Al flux was varied to give different compositions. A linear shutter was used to mask successively larger portions of the substrate as the Al content was reduced. Highly doped n-type GaAs was then deposited over the entire wafer for ease in making ohmic contact. The result was a wafer with three layers of AlGaAs, each with a different Al content, and each lying on top of a layer with about an order of magnitude higher resistivity. Thus, three different AlGaAs compositions could be produced and independently measured in each run. The Al content was determined from the 77K photoluminescence. A point representing one typical MBE GaAs layer doped with Sn to the same level as the GaAlAs is also shown, as is an LPE result[4] and GaAs theoretical maximum curve for comparison. It is seen that the addition of even small amounts of Al rapidly decreases the free electron concentration and the carrier mobility.

The decrease in free carrier density is approximately inversely proportional to the Al content of the layer. In Fig. 6, free carrier

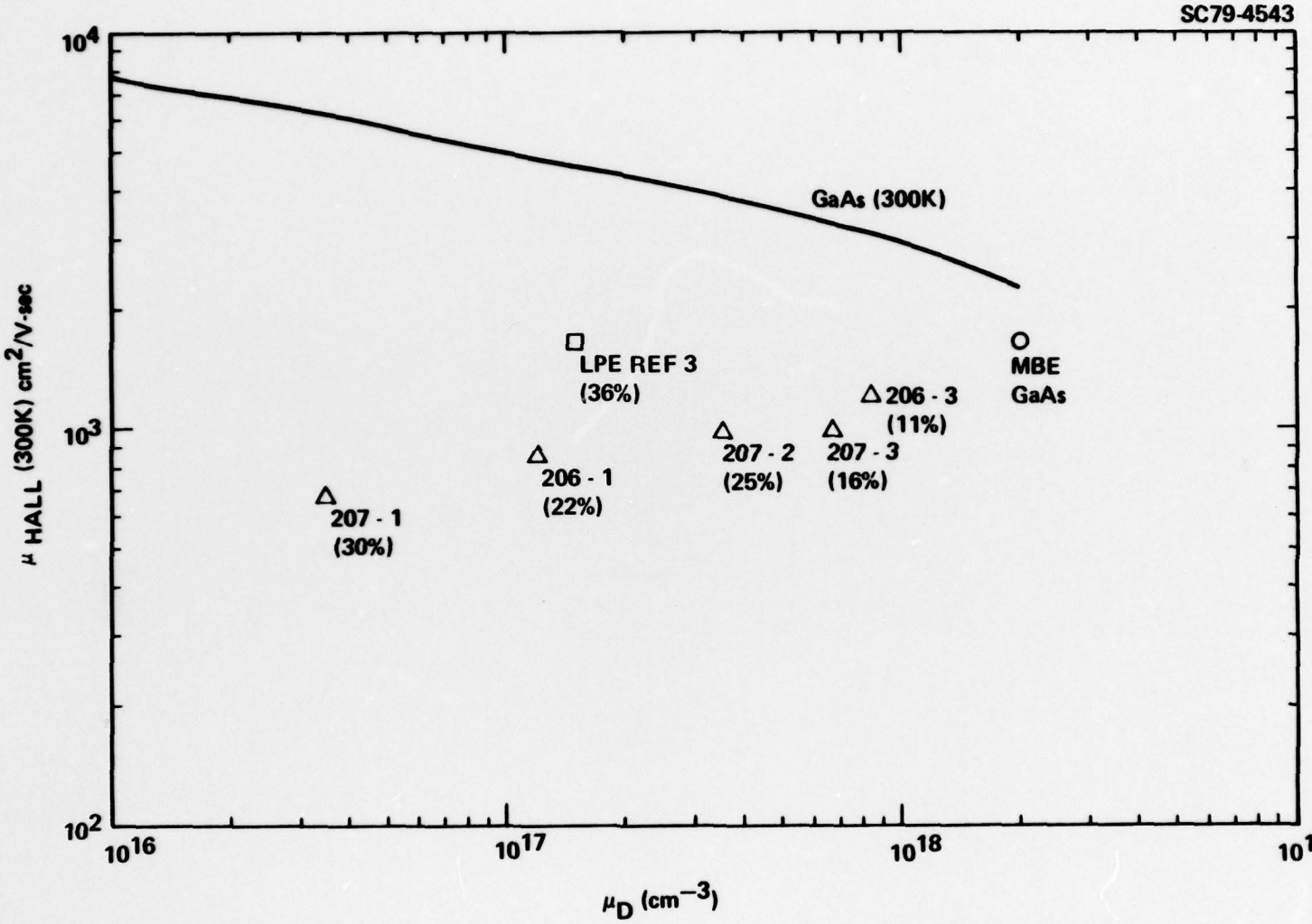

Fig. 5. Electron Hall mobility at 300K as a function of free electron concentration for n-type MBE AlGaAs. Values for LPE AlGaAs and MBE GaAs are included, along with the approximate theoretical maximum for GaAs (solid line). The aluminum content of the layers is given in parentheses below the growth number.

SC5158.2FR

Rockwell International

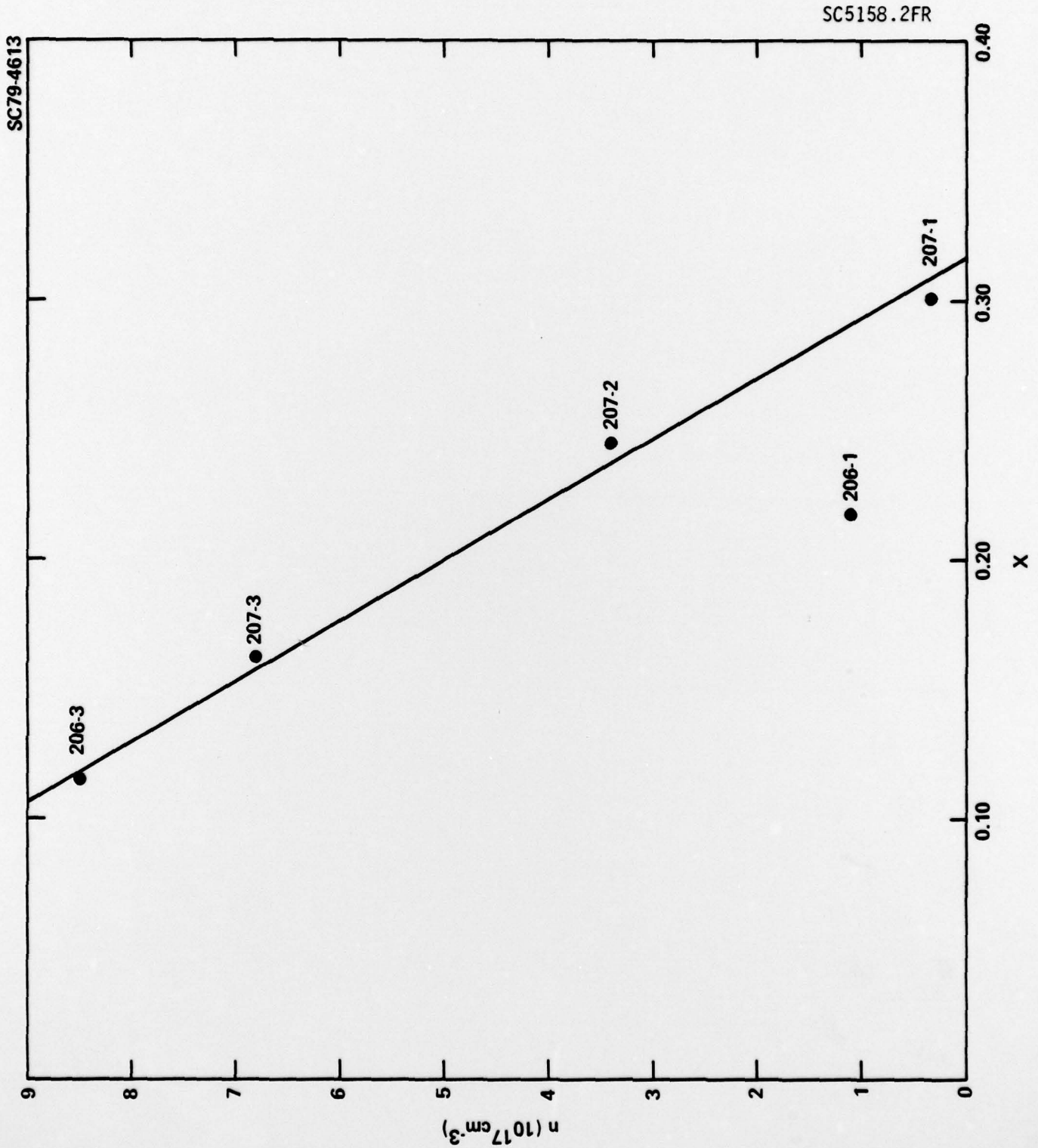

Fig. 6. Free electron density as a function of Al content, for MBE AlGaAs layers containing about 2 x 10^{18}/cm^3 Sn.

density is plotted as a function of Al content for two growth runs. Except for layer 206-1, data for all of the layers lie along a straight line with a slope of $-4.3 \times 10^{18} cm^{-3}$. The zero-Al intercept is $n(0) \cong 1.4 \times 10^{18} cm^{-3}$ in good agreement with the known value of $n(0) = 2 \times 10^{18} cm^{-3}$ obtained from the calibration of n vs. source temperature for the Sn doping source and GaAs layer growth.

Current-voltage measurements were made at room temperature on several of the GaAs/AlGaAs heterojunctions. Ohmic contact in all cases was made to the substrate by the In used to mount the wafers in the MBE chamber. Ohmic contact to the AlGaAs layers was made in a standard way by depositing an Au/Ge alloy onto a heavily doped thin GaAs layer grown on the AlGaAs. This Au/Ge alloy was annealed at about 450°C on a strip heater in flowing H_2 to make the ohmic contact. These contacts were checked for ohmic behavior to the top GaAs layer, then I-V measurements were made across the entire GaAs-GaAlAs-GaAs structure. Figure 7 shows a typical I-V trace. No indication of non-ohmic behavior was observed, even at the lowest current and voltage levels. More measurements at lower temperatures will be made on these layers in the future by Prof. Kroemer.

Some initial C-V measurements were made by Prof. Kroemer on the MBE GaAs/AlGaAs/GaAs n-n-n structures. Figure 8 shows data from one of those measurements. At room temperature, the C-V profile indicated that the AlGaAs layer in this growth had a very low carrier concentration and was depleted at zero bias. This sample also exhibited considerable hysteresis in the capacitance-voltage characteristic, presumably as a result of traps in the AlGaAs layer. Measurements will be made at higher temperatures in an effort to reduce trapping effects.

Photoluminescence measurements were made on a number of AlGaAs layers produced for this contract. The measurements were made at 77K and were used to determine the alloy composition. The aluminum fraction x was determined from the relation:

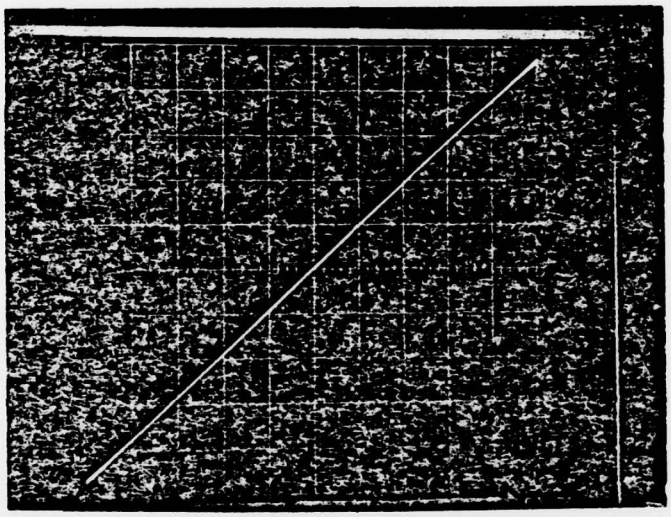

Fig. 7. I-V trace at 300K of a GaAs(n)/$Ga_{.82}Al_{.18}As$(n) heterojunction (sample 206-2). y = 5ma/div.; x = 1v/div.

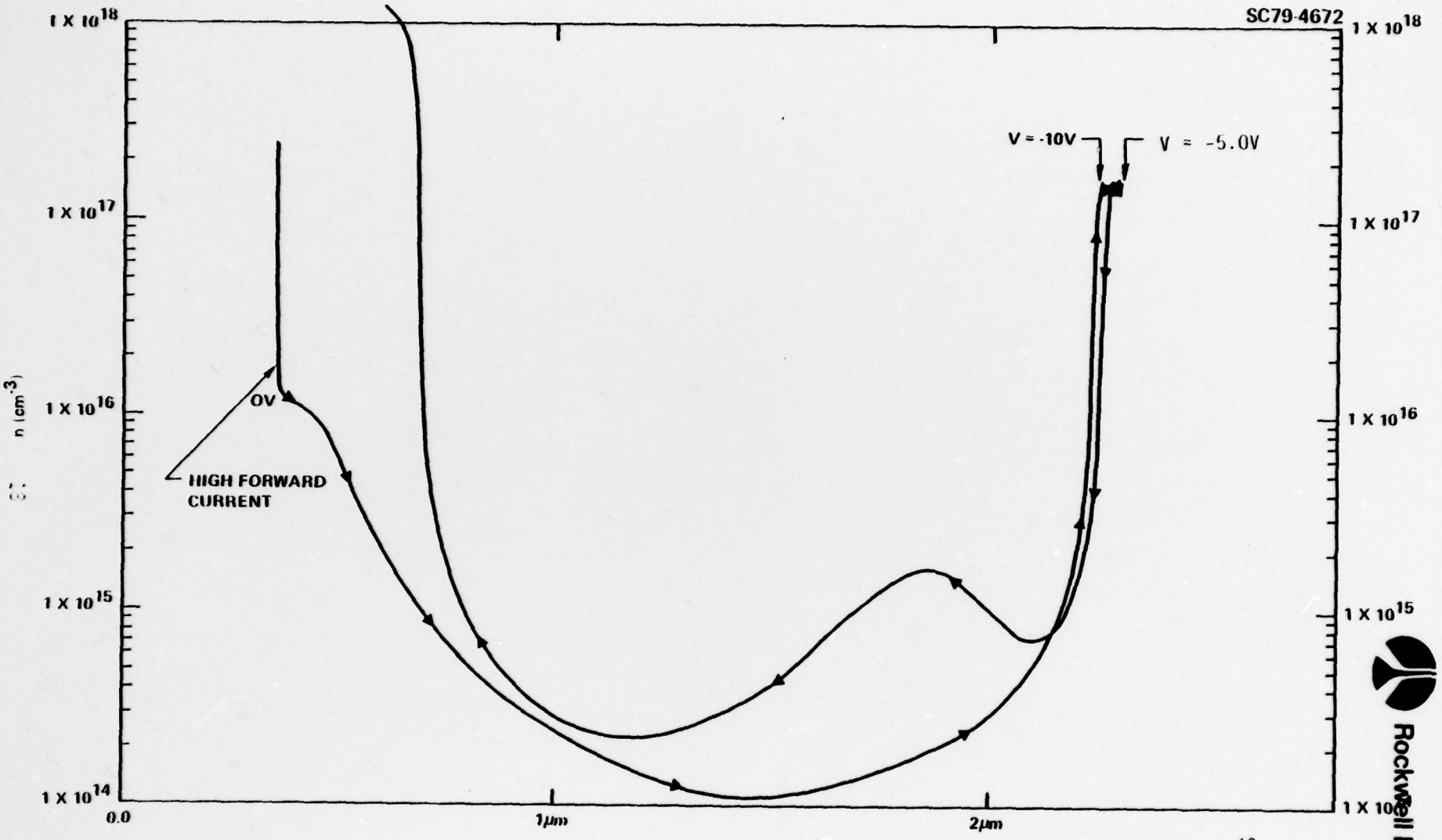

Fig. 8. C-V profile of sample 224, GaAs(Sn)/$Al_{.3}Ga_{.7}As$(Sn)/GaAs(Sn). (Data from H. Kroemer, University of California at Santa Barbara).

$$x(77) = (9569\text{Å})/\lambda(77\text{K}) - 1.163 \quad (1)$$

Equation 1 was obtained from published values for the composition dependence of bandgap, the temperature dependence of the GaAs bandgap, and the composition dependence of the diference between 77K and 300K photoluminescence peaks, i.e.

$$Eg(x, 77\text{K}) = Eg(x,300\text{K}) + \Delta Eg(x), \text{ where} \quad (2)$$

$$\Delta Eg(x) \equiv Eg(x,77\text{K}) - Eg(x,300\text{K}). \quad (3)$$

The composition dependent energy gap was taken to be[5]

$$Eg(x,300\text{K}) = 1.424\text{eV} + 1.247x \text{ eV}. \quad (4)$$

The difference between 300K and 77K photoluminescence peak positions as a function of composition has been reported as

$$\Delta Eg(x) = \Delta Eg(0)\,[1 + 0.6x]^{(6)}. \quad (5)$$

The value of Eg(0) can be obtained from

$$Eg(0,T) = 1.519\text{eV} - (5.405 \times 10^{-4}T^2)(T + 204)^{-1}\text{eV}^{(7)}. \quad (6)$$

Combining Eq. 2-6 gives

$$Eg(x,77) = 1.509\text{eV} + 1.298x \text{ eV}. \quad (7)$$

Converting to wavelength and solving for x gives Eq. 1. Values of compositions obtained from photoluminescence measurements and Eq. 1 are shown in Table 1 with two significant figures; the composition of other layers was estimated from Ga and Al flux measurements.

For a number of layers, two distinct photoluminescent peaks were observed. The wavelength and intensity of these peaks is listed in Table 2. The shorter wavelength peak was assumed to be near-band edge luminescence, while the longer wavelength peak appears to be associated with donor atoms in the GaAlAs. A spectrum of the luminescence from one of the samples is shown in Fig. 9. The level responsible for this luminescence moves further in energy from the band edge as doping density increases, while Al content does appear to decrease the intensity of the luminescence faster than the band edge luminescence, however. This second peak is not seen in all AlGaAs layers, and its origin is not understood.

TABLE 2

Layer	Al%	Position Peak 1	Position Peak 2	Intensity (arb. units) Peak 1	Intensity (arb. units) Peak 2	ΔE(meV)	Doping	Comments
139	21.9	6925	7160	80	165	60	Sn ($\sim 10^{17}/cm^3$)	
206-1	21.7	6932	7430	120-160	350	120	Sn($\sim 2x10^{18}/cm^3$)	
206-2	17.5	7150	7760	145	690	120	Sn($\sim 2x10^{18}/cm^3$)	
206-3	11.6	7480	8000	140	580	110	Sn($\sim 2x10^{18}/cm^3$)	
207-1	30.1	6535	6890	85	175	100	Sn($\sim 2x10^{18}/cm^3$)	
207-2	24.5	6797	7289	175	1240	120	Sn($\sim 2x10^{18}/cm^3$)	
207-3	16.3	7215	7700	~160	1520	110	Sn($\sim 2x10^{18}/cm^3$)	
211	30.3	6525	6836	27	>180	85		Layer grown for another project
218	28.5	6607	6895	~180	1900	80		Est. background n-type dopants $3.5x10^{1}$

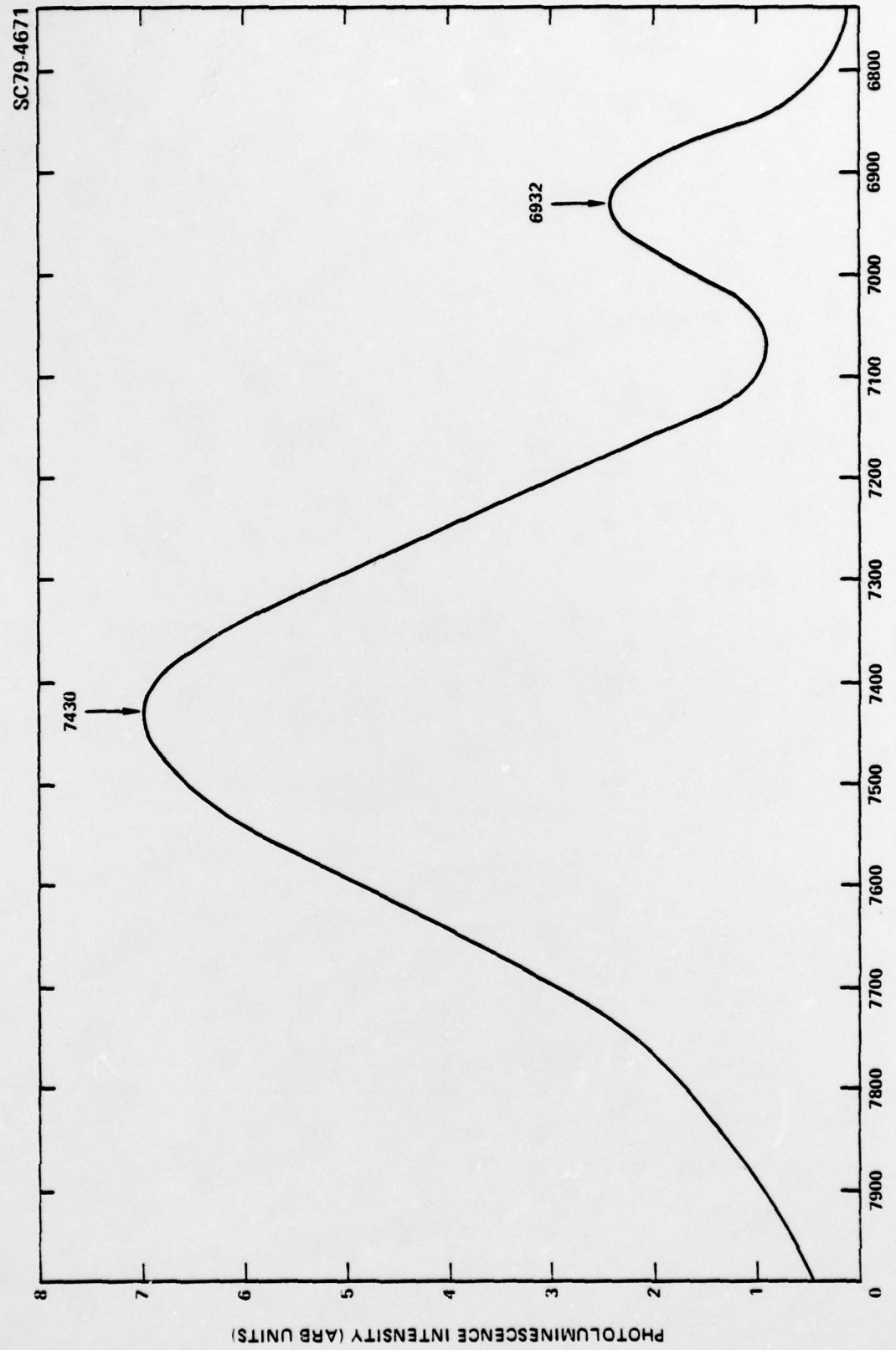

Fig. 9. 77K photoluminescence from sample 206-3 ($Al_{.12}Ga_{.88}As(Sn)$).

3.0 SUMMARY

Molecular beam epitaxy was used to provide samples for extremely abrupt GaAs/GaAlAs heterojunctions for AES profiling of the interface[2] and ESCA measurements of the AlAs valence band structure. The latter samples consist of MBE AlAs layers covered with 50Å to 100Å of GaAs as protection against oxidation. This allows them to be transferred to the ESCA chamber, where a sputter/anneal cycle is used to remove the GaAs and leave a clean AlAs surface. Details of experiments done with these layers will be reported under ONR contract No. N00014-78-C-1109 (R. Grant, principal investigator).

A large amount of effort was used for the study of MBE growth of n-type AlGaAs. This was done to provide material for GaAs(n)/AlGaAs(n) heterojunctions, in an attempt to understand the nature of electrical transport across this interface. N-type AlGaAs was produced although all the n-type conducting AlGaAs layers grown by MBE had low activation of the dopant (2%-4%) and relatively low room temperature mobilities ($650cm^2$/v-sec to $1200cm^2$/v-sec).

Several changes were made to the MBE chamber, which led to the production of conducting n-type AlGaAs. Those which were probably most important concerned the design of the Al and Sn sources. The early Al source design probably produced AlO or Al_2O in the aluminum beam, due to reduction of Al_2O_3 support pieces by the Ta heater wire. This problem was reduced by using a redesigned pyrolytic boron nitride crucible which has a flanged exit end, eliminating possible paths from high temperature heater parts to the substrate. The performance of the Sn doping source was found to change drastically when it was used at high temperatures to produce dopings of greater than $10^{18}/cm^3$. This resulted in a number of layers which were doped much less heavily than planned. The source eventually stabilized after several runs at very high doping levels.

Another factor which undoubtedly influenced the quality of the n-type AlGaAs was the level of residual H_2O, CO and other vacuum contaminants in the chamber. Purchase of a cryogenic pump and modification of the source shrouding to use liquid nitrogen reduced the level of these contaminant gasses by approximately a factor of four.

Some initial measurements were made on the electrical properties of n-GaAs/n-AlGaAs and n-GaAs/n-AlGaAs/n-GaAs structures. I-V measurements on n-n structures at room temperature showed no deviations from ohmic behavior, while C-V measurements on n-n-n structures were hampered by trapping effects in the AlGaAs. The question therefore still is unanswered why some experiments, such as C-V profiling of LPE heterojunctions, indicate a conduction band spike, yet transport measurements do not exhibit rectification.

Photoluminescence spectra of Sn-doped AlGaAs showed two distinct peaks; one peak is near-band edge luminescence, while the second peak appears to be associated with the presence of Sn.

In the future, work will be continued on the growth of the AlAs/GaAs heterojunctions for ESCA valence band discontinuities studies under contract no. N00014-78-C-1109. The samples prepared to date have been satisfactory, and required no special growth procedures.

Several tasks need to be undertaken in order to produce completely satisfactory n-type AlGaAs for heterojunction transport measurements and C-V profiling. Further redesign of the Al source is needed to reduce outgassing. The Sn doping source should be rebuilt for more reliable performance. Other n-type dopants, particularly Si, should be investigated in order to obtain higher dopant activation. The relation between growth parameters (rate, substrate temperature, As/Ga ratio) and the second photoluminescence peak must be investigated for several n-type dopants to understand the relation between the electronic level producing the photoluminescence and the low dopant activation and mobility. The relation of background vacuum to material electronic properties also needs to be explored in the range of vacuum now attainable.

4.0 REFERENCES

1. A. Chandra and L. F. Eastman, data presented at the Physics of Compound Semiconductor Interfaces Conference No. 6, Asilomar, CA., Jan. 1979.

2. C. M. Garner, C. Y. Su, W. E. Spicer, P. D. Edwood, D. Miller and J. S. Harris, Appl. Phys. Lett. 34, 610 (1979).

3. R. F. C. Farrow and G. M. Williams, Thin Solid Films 55, 303 (1978).

4. R. J. Nelson, Appl. Phys. Lett. 31, 351 (1977).

5. Heterostructure Lasers, Part A, H. C. Casey, Jr. and M. B. Panish, Academic Press, 1978, p. 193.

6. F. M. Vorobkalo, K. D. Clinchuk, and V. F. Kovalenko, Sov. Phys. Semicond. 9, 656 (1975).

7. Heterostructure Lasers, Part B, H. C. Casey, Jr. and M. B. Panish, Academic Press, 1978, p. 9.